BMC Genomics

RESEARCH

Open Access

Transcriptome integration analysis revealed that miR-103-3p regulates goat myoblast proliferation by targeting *FGF18*

Kunyu Li[1†], Yize Song[1†], Yekai Fan[1], Hui Zhang[1], Mingxing Chu[1*] and Yufang Liu[1*]

Abstract

Background Myoblasts serve as the fundamental building blocks of muscle fibers, and there is a positive correlation between the diameter of myofibers during the juvenile phase and the rate of muscle growth, which does not change in adulthood. However, the molecular mechanisms governing myofiber diameter across various developmental stages in goats remain largely unclear.

Results In this study, we examined miRNA expression in the *longissimus dorsi* muscle tissue of goats at two distinct ages: one month, a period characterized by robust muscle growth, and nine months, when muscle development plateaus in adulthood. A total of 408 known miRNAs and 86 novel miRNAs were identified, with 32 miRNAs exhibiting differential expression between the two groups. A functional enrichment analysis of these targeted genes revealed significant enrichment in pathways closely correlated with skeletal muscle growth, development, and senescence. Notably, chi-miR-103-3p was identified among the DE miRNAs and appeared to play an important role in skeletal myoblast proliferation. Bioinformatics analysis, complemented by dual luciferase activity assays revealed that chi-miR-103-3p specifically targets the 3'UTR of *FGF18*. Subsequent cell transfection experiments demonstrated that chi-miR-103-3p suppresses the expression of *FGF18* in goat myoblasts, thereby inhibiting cell proliferation. Moreover, *FGF18* was observed to enhance the proliferation of goat myoblasts.

Conclusions Collectively, our data indicated that the elevated expression of chi-miR-103-3p in adult goat myoblasts significantly repressed *FGF18* expression, thereby limiting rapid muscle growth. Proliferation and differentiation of myoblasts can affect myofiber number and cell volume expansion. These findings lay the foundation for further elucidation of the molecular mechanisms underlying muscle growth and development across different life stages of goats. Additionally, it could be a potential molecular marker for improving muscle production in goats.

Keywords Goat, miRNA-seq, Skeletal myoblast proliferation, chi-miR-103-3p, *FGF18*

[†]Kunyu Li and Yize Song contributed equally to this work.

*Correspondence:
Mingxing Chu
mxchu@263.net
Yufang Liu
aigaiy@126.com
[1]State Key Laboratory of Animal Biotech Breeding, Institute of Animal Science, Chinese Academy of Agricultural Sciences, Beijing 100193, China

Introduction

Since the dawn of the 21st century, goat farming has gained significant popularity in the livestock breeding sector. The cholesterol content of goat meat is notably lower than that of sheep meat, which can contribute to the prevention of conditions such as vascular sclerosis and heart disease. This makes it an ideal choice for individuals with elevated blood lipid levels and for elderly individuals. Additionally, goat farming aligns with the contemporary demand for a variety of dietary options [1–5]. However, there is a dearth of comprehensive research on the molecular mechanisms driving muscle proliferation and development in goats. The muscle growth and development of goats vary with age. Studies on sheep have revealed that the diameter of the muscle fibers of the longest dorsal muscle increases with age. Similarly, in lambs, the diameter of *longissimus dorsi* tissues begins to increase after birth (at approximately 1 month of age), and this growth ceases by the age of nine months [6, 7]. Muscle fiber growth and development are intricate and involve the interplay of various genetic elements and signaling cascades. Within the Wnt signaling pathway, Myf5 (myofactor-5, myogenic factor 5 of the basic helix-loop-helix family of proteins) and Myod (myogenic terminator gene, myogenic determinant of proliferation and differentiation of myoblasts) are activated and expressed, promoting the maturation of muscle precursor cells into myoblasts. These myoblasts then coalesce to create myotubes, which ultimately differentiate into myofibers [8]. To gain deeper insight into muscle growth, disease mechanisms, and gene expression in goats, characterizing muscle development at different ages is essential.

MicroRNAs (miRNAs) are instrumental in the epigenetic modulation of numerous biological processes that govern gene expression [9]. The miRNAs modulate gene expression by binding to the 3' untranslated region (3'UTR) of target genes, leading to mRNA cleavage or repression of translation [10]. Muscle-specific miRNAs, such as miR-1, miR-133a/b, and miR-206, regulate myogenic cell proliferation and differentiation by targeting genes such as histone deacetylase 4 (HDAC4), serum response factors (SRFs), and the myogenic differentiation family [11–13]. Concurrently, nonmuscle-specific miRNAs, including miR-17, miR-19, miR-15b, miR-322, miR-208b, miR-26a, miR-30, miR-128a, miR-203a, miR-214, and miR-3906, also play significant roles in the regulation of muscular development and maturation [14–17]. For example, miR-3906 and miR-203a modulate rapid muscle differentiation by specifically targeting Hmer-1b and Dmrt2a, respectively [18, 19]. The miR-26a promotes the proliferation and differentiation of myogenic cells by modulating the expression of Smad1 and Smad4 [20]. During the aging of skeletal muscle, miRNAs such as let-7, miR-29, miR-99, miR-100, miR-451, miR-144, miR-18a, and miR-181 are involved in regulation [21–23]. Notably, let-7b and let-7e from the let-7 miRNA family are upregulated in aging skeletal muscle, where they regulate cell cycle processes of their target genes, including proliferation and differentiation [24].

In this research, the objective was to identify miRNAs with varying expression levels that affect myofiber proliferation at different developmental stages in goats through deep sequencing. Additionally, we aimed to explore the expression patterns and target genes of key regulatory miRNAs. Based on miRNA sequencing and target gene prediction results, the candidate miRNA chi-miR-103-3p and its target gene fibroblast growth factor 18 (*FGF18*) were identified as potential factors associated with the development of goat myofibers and the proliferation of myoblasts. We then conducted further functional validation of miR-103-3p and *FGF18*. Our results provide insights into the molecular mechanisms of goat myofiber growth and development and offer new directions for subsequent studies.

Materials and methods

Animals and sample collection

Goats come from the goat breeding farm in Wu'an city, Hebei Province, China, were cultivated under consistent conditions. Three 1-month-old (mon1) and three 9-month-old (mon9) healthy Wu'an goats were selected by the same rearing method, and their *longissimus dorsi* tissues were collected. Tissue samples from the *longissimus dorsi* muscle were collected, immediately enclosed in sterile RNase-free Eppendorf tubes, rapidly frozen in liquid nitrogen, and then sent to the laboratory for storage at -80 °C until the total RNA extraction procedure was initiated.

Small RNA sequencing and data analysis

Using the Illumina small RNA sample preparation kit, we constructed two distinct small RNA libraries derived from the *longissimus dorsi* muscle tissues of Wu'an goats aged 1 month and 9 months. In brief, we isolated and purified 16–35 nt fragments from a PAGE gel and then ligated adapters to their respective 5' and 3' ends using T4 RNA ligase. The resulting products, after RT–PCR amplification, were 140–160 bp PCR amplicons, which were further purified on 8% polyacrylamide (100 V, 80 min). The purified cDNA fragments were sequenced on an Illumina HiSeq 2500 platform. Postprocessing steps included the elimination of poly-N sequences, 3' and 5' adaptor contamination, and the exclusion of reads containing only a single nucleotide (A, T, G, or C), as well as fragments shorter than 18 nucleotides. This resulted in the production of 50 bp single-end reads from the raw data. The clean reads were compared to the *Capra hircus* Genome assembly ARS1.2 (https://www.ncbi.nlm.nih.g

ov/datasets/genome/GCF_001704415.2/) by Bowtie to annotate all known rRNA, tRNA, scRNA, snRNA, and snoRNA small RNA sequences. The DEG seq R package was used to analyze the differentially expressed (DE) miRNAs according to the normalized transcripts per kilobase per million reads (TPM) values. The DE miRNAs were identified with q-value < 0.01 and |log2 (fold change) |>1 as the thresholds.

Prediction of differential miRNA target genes and gene ontology (GO) and kyoto encyclopedia of genes and genomes (KEGG) analyses

The target genes of the DE miRNAs were identified using the TargetScan (http://www.targetscan.org/) and miRanda (microRNA.org) databases, while visual network maps were created with Cytoscape 3.1.0 (http://www.cytoscape.org/). To further explore the biological functions and metabolic pathways associated with DE miRNAs and their targets, we conducted GO and KEGG analyses (http://geneontology.org) using the DAVID Bio informatics Resources v6 (http://david.abcc.ncifcrf.gov/) and KOBAS (http://kobas.cbi.pku.edu.cn/index.php), respectively.

Reverse transcription (RT) - qPCR validation

To confirm the accuracy of the sequencing results, we selected 10 DE miRNAs for validation through RT-qPCR. Approximately 0.1 μg of total RNA was used for each sample and reverse transcribed to cDNA using RT reagent (Thermo Fisher Scientific, Waltham, MA, USA). U6 small nuclear RNA functioned as an internal control for standardizing the expression levels of the target genes, and all experiments were conducted three times to ensure reliability. RT-qPCR was performed on a LightCycler 480II (Roche, Basel, Sweden) using SYBR Premix Ex Taq II. The procedure consisted of predenaturation for 5 s at 95 °C, followed by 40 cycles of denaturation at 95 °C for 5 s, annealing at 60 °C for 30 s, extension at 72 °C for 5 s, and storage at 4 °C. After completion of the reaction, melting curve analysis was performed. Relative expression levels were determined using the $2^{-\Delta\Delta Ct}$ method. *P* values were calculated by *t* test, and $P<0.05$ was considered to indicate a significant difference. The miRNA primers were designed using the plus-tail method, and the primer sequences are shown in Table 1.

Western blotting

Proteins from cells and tissues were extracted with RIPA buffer (Solarbio, Beijing, China). The cells were collected and centrifuged at 4 °C at a speed of 12,000 r/min for 10 min after RIPA buffer was applied to the cell culture plates. Protein concentrations were assessed using a BCA protein assay kit (Solarbio, Beijing, China). Then, the supernatant was combined with 1/4 the volume of loading buffer and denatured. The specific assay was described by Yao [25]. The primary antibodies used were against FGF18 (1:100, SANTA, USA), CDK4 (1:100, CST, USA), Cyclin D2 (1:100, CST, USA), and β-tubulin

Table 1 Primers used in this study

Name	Primer sequence (5′-3′)	Tm (℃)	Usage
miR-93-3p	ACTGCTGAGCCAGCACTTCC	60	miRNAs quantitative upstream primers
let-7e-5p	CGGTCTGGGTGAGGTAGGAG	60	miRNAs quantitative upstream primers
miR-103-3p	GAGCAGCATTGTACAGGGCTATG	60	miRNAs quantitative upstream primers
miR-1224	GTGAGGACTCGGGAGGTGG	60	miRNAs quantitative upstream primers
miR-21-3p	AACAGCAGTCGATGGGCTGT	60	miRNAs quantitative upstream primers
miR-346-5p	GTCTGTCTGCCCGCATGCCTGCCTC	60	miRNAs quantitative upstream primers
Novel-466	AGCCGCGTGCTTTC	60	miRNAs quantitative upstream primers
miR-1307-3p	GACTCGGCGTGGCGTCGGTCGTG	60	miRNAs quantitative upstream primers
miR-211	GCAGTTCCCTTTGTCATCCT	60	miRNAs quantitative upstream primers
miR-27a-5p	AGGGCTTAGCTGCTTGT	60	miRNAs quantitative upstream primers
U6	CAAGGATGACACGCAAATTCG	60	miRNAs quantitative upstream primers
universal downstream primer	GTGCAGGGTCCGAGGT	60	Universal downstream primers for miRNAs and U6 internal reference
FGF18	F: GAAGCAGGTGAAGATGCCAGT	60	primers of FGF18 for real-time PCR
	R: CTTGTTGAAATAAAAGCCCCTG		
CDK4	F: GAGCATCCCAATGTTGTCAGG	60	primers of CDK4 for real-time PCR
	R: ACTGGCGCATCAGATCCTTT		
Cyclin-D1	F: GCCACAGACGTGAAGTTCATTT	60	primers of Cyclin-D1 for real-time PCR
	R: CGGGTCACATCTGATCACCTT		
Cyclin-D2	F: ATGTGGATTGCCTCAAAGCC	60	primers of Cyclin-D2 for real-time PCR
	R: CAGGTCGATATCCCGAACATC		
RPL19	F: ATCGCCAATGCCAACTC	60	house-keeping gene, primers of RPL19 for real-time PCR
	R: CCTTTCGCTTACCTATACC		

(1:1000, SANTA, USA). The secondary antibodies used were goat anti-mouse (1:5000, Proteintech, USA) and goat anti-rabbit (1:5000, Proteintech, USA) secondary antibodies. Detection was performed using Image Lab™ (Bio-Rad, Berkeley, USA) chemiluminescent immunoblotting substrate (Santa Cruz, USA). The blots used in the images are untreated and they come from different parts of the same gel. Protein band intensities were quantified using ImageJ software.

In vitro isolation and culture of goat myoblasts

Goat *longissimus dorsi* tissues were minced into small pieces and rinsed 3–5 times with a phosphate-buffered saline (PBS) solution containing 2% triple antibody. The tissues were then diced to approximately 1 mm^3 in size, treated with 0.25% trypsin (containing 0.05% EDTA) and placed in a refrigerator at 4 °C overnight. The enzymatic digestion process was terminated by introducing DMEM/F12 medium enriched with 10% FBS and then incubating at 37 °C for a period of 1 h. The cells were gently blown with a pipette until the tissue pieces basically disappeared, followed by sequential filtration through 200-mesh and 400-mesh cell strainers. The filtrate was collected by centrifugation at 3000 ×g for 5 min, and the cell precipitate was collected and washed by centrifugation with cell culture medium once. The cell culture medium (DMEM/F12+10% FBS+1% triple antibody) was resuspended, and the cells were inoculated into culture bottles and incubated in an incubator at 37 °C, 5% CO_2 and air-saturated humidity. The HEK293T cell line, obtained from our laboratory, was cultured under the same conditions and used for the dual luciferase activity assay.

Plasmid construction

The wild-type (WT) and mutant (MUT) fragments of the *FGF18* 3'UTR were cloned and inserted into the pmirGLO vector. The recombinant plasmids used were FGF18-UTR-WT and FGF18-UTR-MUT. The pcDNA3.1-FGF18 vector was constructed by inserting the coding region of goat *FGF18* into the pcDNA3.1-EGFP vector, with pcDNA3.1-EGFP serving as a negative control (NC). We used Sigma's pLKO.1-puro shRNA vector to construct an interference plasmid targeting *FGF18*. Three shRNA plasmids were designed, and their interference efficiency was verified through cell transfection experiments. The plasmid with the highest interference efficiency was selected for subsequent functional validation. The shRNA sequences are shown in Supplementary Table S1. The plasmids were extracted using a QIAGEN Plasmid Midi Kit (QIAGEN, Germany).

Dual luciferase activity assays

The HEK293T cell line was utilized to determine whether miR-103-3p targets the 3'UTR of *FGF18*. Cells were plated in 24-well plates and grown to 70% or greater confluence before transfection. A total of 500 ng of either FGF18-UTR-WT or FGF18-UTR-MUT, along with 2 μL of chi-miR-103-3p mimics, was transfected using Lipofectamine 2000 (Invitrogen), with an empty vector serving as a negative control. The luminescence of luciferase was quantified 48 h posttransfection using a dual-luciferase assay system (Promega, WI, USA). The assay was performed in triplicate.

Cell proliferation assay

Goat myoblasts were seeded into 96-well plates, and their growth was evaluated after transfection with a CCK-8 Cell Proliferation and Cytotoxicity Assay Kit (Solarbio Technology, Beijing, China). At 6 h post-transfection, the medium was changed, and 10 μL of CCK-8 reagent was added to each well. The cells were then incubated in a cell incubator for 2 h, after which they were treated for an additional period, and subsequently, the absorbance was determined at a wavelength of 450 nm using a microplate spectrophotometer (Thermo Fisher, Varioskan LUX, USA) after 0, 6, 12, 24 and 48 h of incubation.

The proliferation status of the myoblasts was assessed using EdU with the CBeyoClick™ EdU-488 Cell Proliferation Assay Kit (Beyotime, China) following the manufacturer's protocol. A 6-well plate was used, and each well received a final concentration of 10 μM EdU for a 6 h incubation in a cell culture incubator. After incubation, the cells were washed three times with PBS and fixed for 15 min at room temperature, after which the fixative was removed. The Ce PBS lls were rinsed three times with a washing solution before treatment with 1 mL of 0.3% Triton X-100 in PBS for 15 min at room temperature to enhance cell membrane permeability. Then, 500 μL of the prepared Click reaction solution was added to each well, and the cells were incubated at room temperature for 30 min in the dark to observe and quantify the number of cells stained with EdU. Three random areas were selected for statistical analysis.

Statistical analysis

The relative mRNA expression levels were determined using RT–qPCR data and the $2^{-\Delta\Delta Ct}$ method. The data are presented as the mean ± standard error (SE) and were derived from a minimum of three separate experiments. GraphPad Prism version 8.02 (GraphPad Software, USA) was used for graphical representation of the data. To assess the statistical significance of differences between groups, Student's *t* test was conducted at the 5% significance level using SPSS 19.0 software (IBM, Chicago, IL,

Table 2 Overview of post-quality control metrics for miRNAs

Sample	Raw reads	Q30	Clean reads	Total mapped sRNA	Uniq reads
			Clean reads rate (%)		
mon1_1	15,533,857	95.60%	14,307,111 (92.10%)	13,159,074 (94.33%)	461,649
mon1_2	14,760,444	95.57%	13,719,869 (92.95%)	11,713,233 (87.63%)	562,541
mon1_3	15,056,352	95.59%	13,817,984 (91.78%)	12,230,121 (91.46%)	709,994
mon9_1	18,223,027	97.24%	17,907,122 (98.27%)	16,330,136 (93.35%)	457,204
mon9_2	15,914,343	97.12%	15,601,318 (98.03%)	13,817,700 (92.86%)	539,245
mon9_3	14,043,436	95.75%	12,978,751 (92.42%)	10,609,736 (89.85%)	713,127

Note Mon1 represents a 1-month-old goat, and Mon9 represents a 9-month-old goat

Table 3 Summary of miRNA identification statistics per library

Types	Total	mon1_1	mon1_2	mon1_3	mon9_1	mon9_2	mon9_3
known miRNA	408	391	366	381	373	361	366
Mapped mature							
Mapped hairpin	256	247	240	243	243	240	240
Mapped uniq sRNA	20,796	3930	3083	3605	3732	3418	3028
Mapped total sRNA	41,864,034	7,347,163	4,196,676	6,737,044	10,182,568	7,359,718	6,040,865
Novel miRNA	86	60	54	65	64	62	55
Mapped mature							
Mapped star	36	22	15	22	23	18	21
Mapped hairpin	89	62	57	67	66	64	61
Mapped uniq sRNA	1372	256	175	263	277	213	188
Mapped total sRNA	38,784	11,797	1958	10,685	7744	4139	2461

USA). A *P* value of less than 0.05 was set as the threshold for statistical significance.

Results

Library sequencing and quality control

From the six small RNA libraries obtained from the *longissimus dorsi* tissue of Wu'an goats (mon1 and mon9 groups), we acquired the following raw reads: 15 533 857, 14 760 444, 15 056 352, 18 223 027, 15 914 343, and 14 043 436 (Table 2). The quality of the RNA-seq data, as measured by the Q30 values, was meticulously maintained between 95.57% and 97.24%. After filtering, we obtained final high-quality, pure reads of 14 307 111, 13 719 869, 13 817 984, 17 907 122, 15 601 318, and 12 978 751 from the respective small RNA libraries of the mon1 and mon9 groups. The majority of these small RNAs had lengths of 21 to 24 nt. Moreover, small RNA sequences spanning from 18 to 35 nt were mapped onto the goat genome sequence, with approximately 87.63–94.33% of the clean reads successfully aligning to the reference goat genome. These mapped sequences were subsequently used for miRNA identification.

miRNAs expression profile in goat *longissimus dorsi* tissue

The clean reads containing tRNA, rRNA, snoRNA and other snRNA sequences were eliminated based on category annotation. The remaining sequences were then mapped to the mature sequences of miRNAs from goats as listed in miRBase (Release 22.0). There were 20,796 unique sequences (41,864,034 reads) that matched exactly with the goat miRNAs (Table 3). With the aid of structure prediction for precursor sequences, a total of 408 known miRNAs and 86 novel miRNAs were identified from the goat *longissimus dorsi* tissue (Supplementary Table S2).

Additionally, we analyzed the expression profiles of 494 miRNAs during various developmental phases in goat *longissimus dorsi* tissue. Of these, 448 miRNAs were expressed at both stages, while 26 and 20 miRNAs were specifically expressed in the mon1 and mon9 groups, respectively (Fig. 1A). These results indicated that the miRNA expression profiles vary among different developmental stages of the goat *longissimus dorsi* muscle. Furthermore, there was a disparity in the abundance of the identified miRNAs, with the majority of the novel miRNAs expressed at relatively low levels in the *longissimus dorsi* samples. In the mon1 and mon9 groups, miRNAs with a TPM>60 constituted an average of 32.52% and 28.61%, respectively, suggesting higher miRNA expression abundance in 1-month-old Wu'an goats than in 9-month-old goats. The identified miRNAs were subsequently categorized into families. The analysis revealed that 277 miRNA precursors were classified into 161 distinct miRNA families. Notably, 18 of these families included more than two precursors. Specifically, the miR-154 family was particularly prominent, with 19 members identified in the *longissimus dorsi* tissue. Additionally, the miRNA families let-7, miR-30, miR-15, miR-10, miR-17,

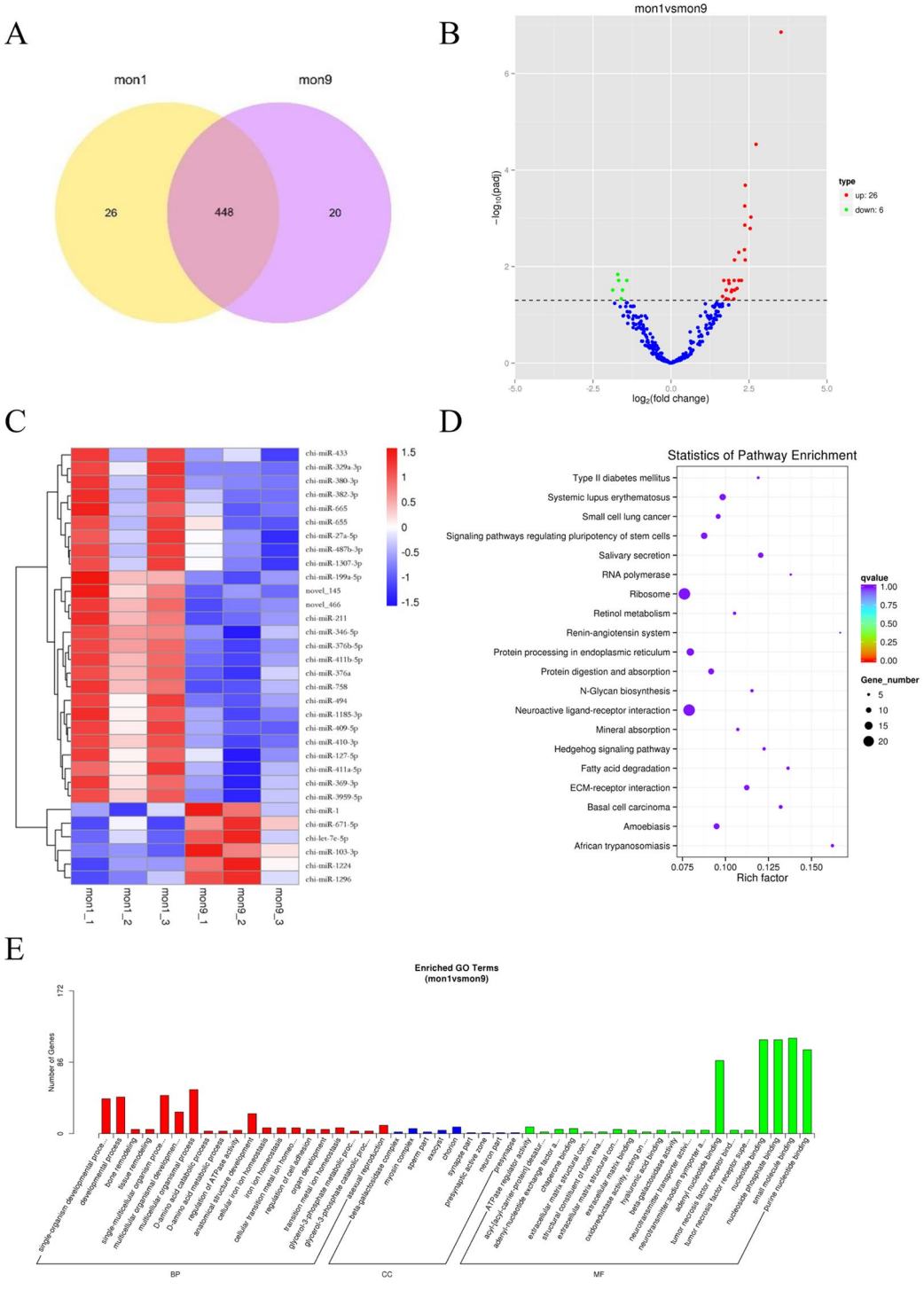

Fig. 1 The results of miRNA-seq analysis. (**A**) Venn diagram of two developmental-stage miRNAs in goat *longissimus dorsi* tissue. (**B**) Volcano plot of differentially expressed miRNAs; red represents upregulated miRNAs, and green represents downregulated miRNAs. (**C**) Differential miRNA clustering heatmap; red represents highly expressed miRNAs, and blue indicates miRNAs with low expression. (**D**) Results of KEGG enrichment. (**E**) The top 20 GO terms enriched in the comparison group

and miR-368 contained 10, 6, 5, 7, 8, and 5 miRNA precursors, respectively.

Significant differentially expressed miRNAs (DEMs) in goat *longissimus dorsi* tissue at two developmental stages

We compared the miRNA expression levels in the *longissimus dorsi* muscle tissue of 1-month-old and 9-month-old Wu'an goats. A total of 32 DEMs were identified when the criteria of q value < 0.01 and | log2 (fold-change)|> 1 were applied (Supplementary Table S3). In the mon1 group, 26 miRNAs were upregulated, and 6 were downregulated (Fig. 1B). A heatmap depicted the distinct miRNA expression profiles between the two developmental stages (Fig. 1C). Cluster analysis revealed that the differentially expressed miRNAs could differentiate between the mon1 and mon9 groups, with similar miRNA expression patterns within the same group. These findings suggested that DEMs were likely closely associated with the growth and development of the *longissimus dorsi* muscle in goats across various stages.

GO and KEGG enrichment analyses of differentially expressed genes (DEGs)

We utilized miRanda and RNAhybrid software to predict miRNA target genes, with the final results derived from the consensus of both programs. To reveal the possible roles of DEGs, we performed analyses using GO terms and pathways from the KEGG database. In the GO analysis (Fig. 1E), the biological process (BP) category was predominantly represented by terms such as multicellular organism process (GO: 0032501) and single-organism multicellular process (GO: 0044707). The cellular component (CC) category was most enriched for terms related to the chorionic villus (GO: 0042600). Within the molecular function (MF) category, the most prevalent terms were associated with small molecule binding (GO: 0036094), nucleotide binding (GO: 0000166), phosphoriboside binding (GO: 1901265), and purine nucleotide binding (GO: 0017076). KEGG analysis indicated that the neuroactive ligand–receptor interaction pathway (chx04080) was the most significantly enriched pathway, along with pathways regulating stem cell pluripotency (chx04550) and protein processing in the endoplasmic reticulum (chx04141) (Fig. 1D). Additionally, the renin-angiotensin system (chx04614) was identified as the most enriched gene pathway.

RNA-seq data validation by RT-qPCR

For RT-qPCR verification, we selected 10 miRNAs, comprising 5 that were upregulated (miR-346-5p, novel-466, miR-1307-3p, miR-211, and miR-27a-5p) and 5 that were downregulated (miR-671-5p, let-7e-5p, miR-103-3p, miR-1224, and miR-1296). The RT-qPCR validation results were consistent with the sequencing data, confirming the reliability of our findings (Fig. 2).

Analysis of the miRNA–mRNA interaction network

To thoroughly investigate the potential functions of miRNAs and their targets in muscle development, we identified a total of 317 genes that were negatively correlated with DEMs and constructed an interaction network for these targets and miRNAs (Supplementary Table S4). Within this network, miR-127-5p, miR-199a-5p, miR-433, miR-665, miR-346-5p, miR-1307-3p, miR-211, novel_145, novel_466, and miR-27a-5p were central and exhibited upregulated expression (Fig. 3A). Conversely, miR-671-5p, miR-103-3p, miR-1296, and miR-1 were central to the miRNA–mRNA network and were downregulated (Fig. 3B). These core miRNAs and their corresponding target genes may serve as key candidates for further functional validation in subsequent studies.

miR-103-3p inhibited the proliferation of myoblasts

Within the miRNA–target gene interaction network, miR-103-3p has emerged as a central miRNA, prompting us to validate its impact on goat myoblast proliferation.

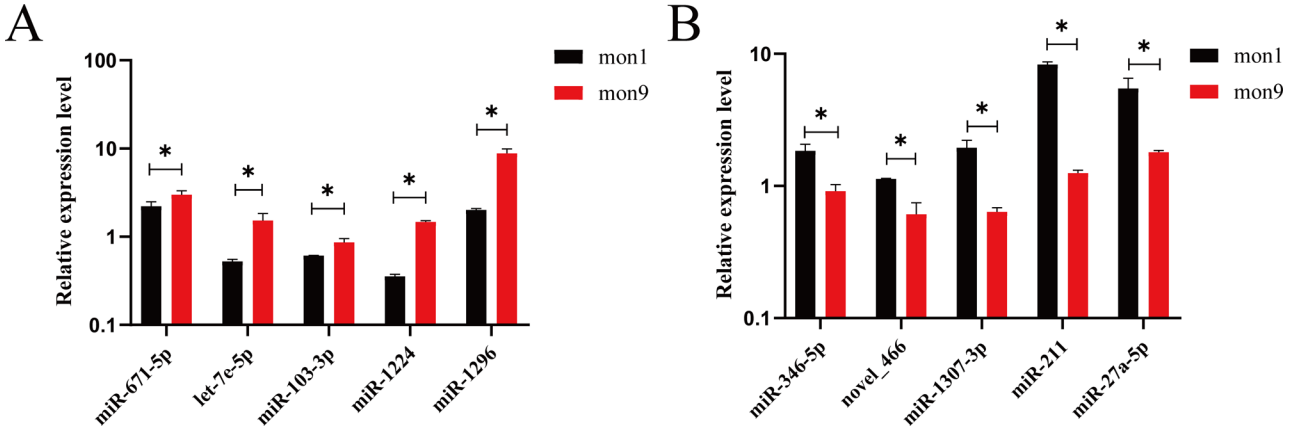

Fig. 2 Verification of differentially expressed miRNAs by RT-qPCR. *$P < 0.05$, **$P < 0.01$

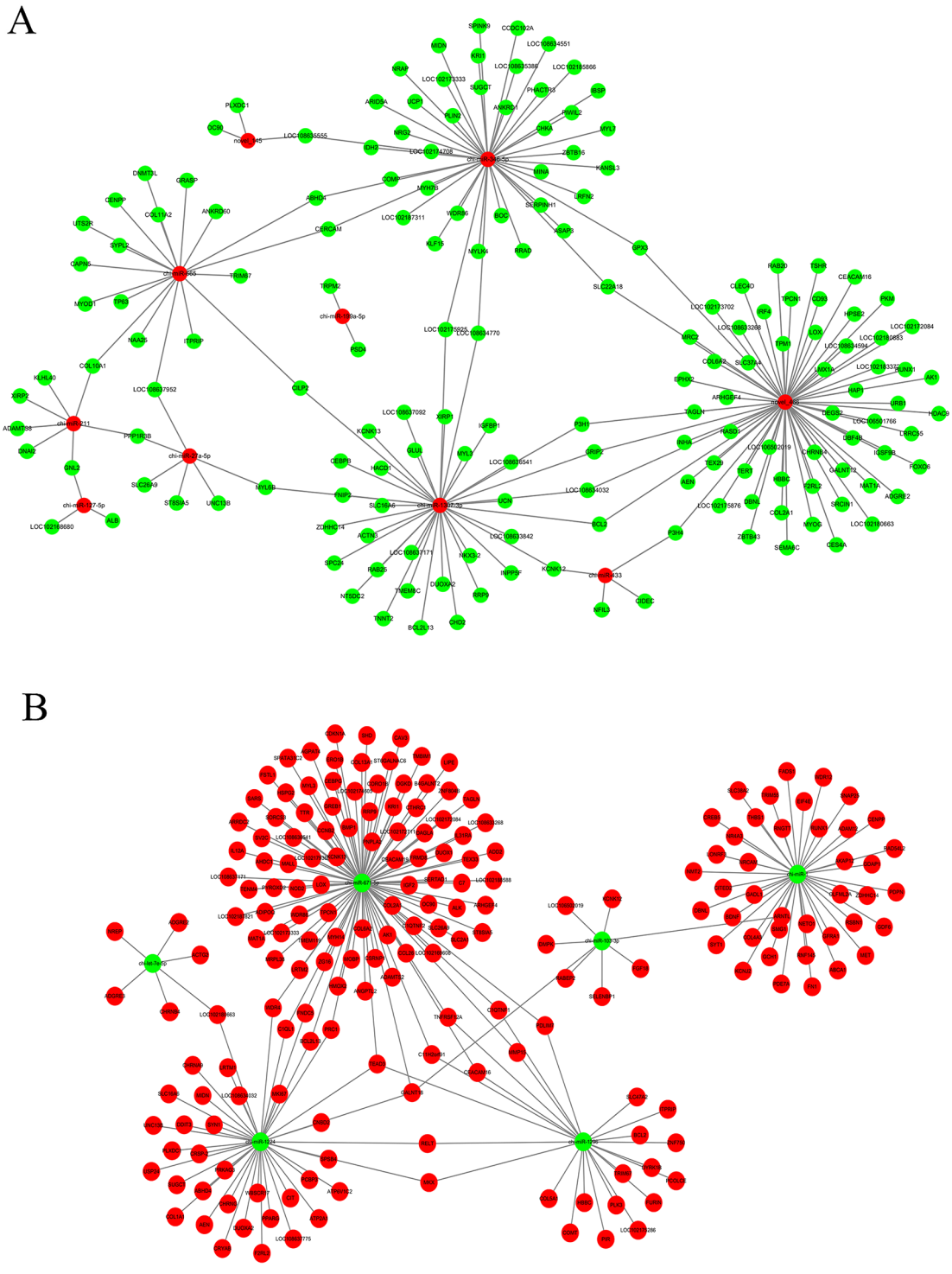

Fig. 3 The miRNA–mRNA network diagram. The red in the figure indicates upregulated genes/miRNAs, and the green indicates downregulated genes/miRNAs. (**A**) Upregulation of miRNAs and downregulation of target genes. (**B**) Downregulation of miRNAs and upregulation of target genes

To determine the effect of miR-103-3p on myoblast proliferation, we transfected cells with miR-103-3p mimics and inhibitors to assess the effects of these treatments on cell proliferation-related genes and the overall cell proliferation rate. RT−qPCR analysis revealed that the relative expression levels of *CDK4*, *Cyclin-D1*, and *Cyclin-D2* in the goat myoblasts significantly decreased when miR-103-3p was overexpressed, and the opposite effect was observed upon its inhibition ($P<0.05$) (Fig. 4A and B). Western blot analyses corroborated the RT−qPCR

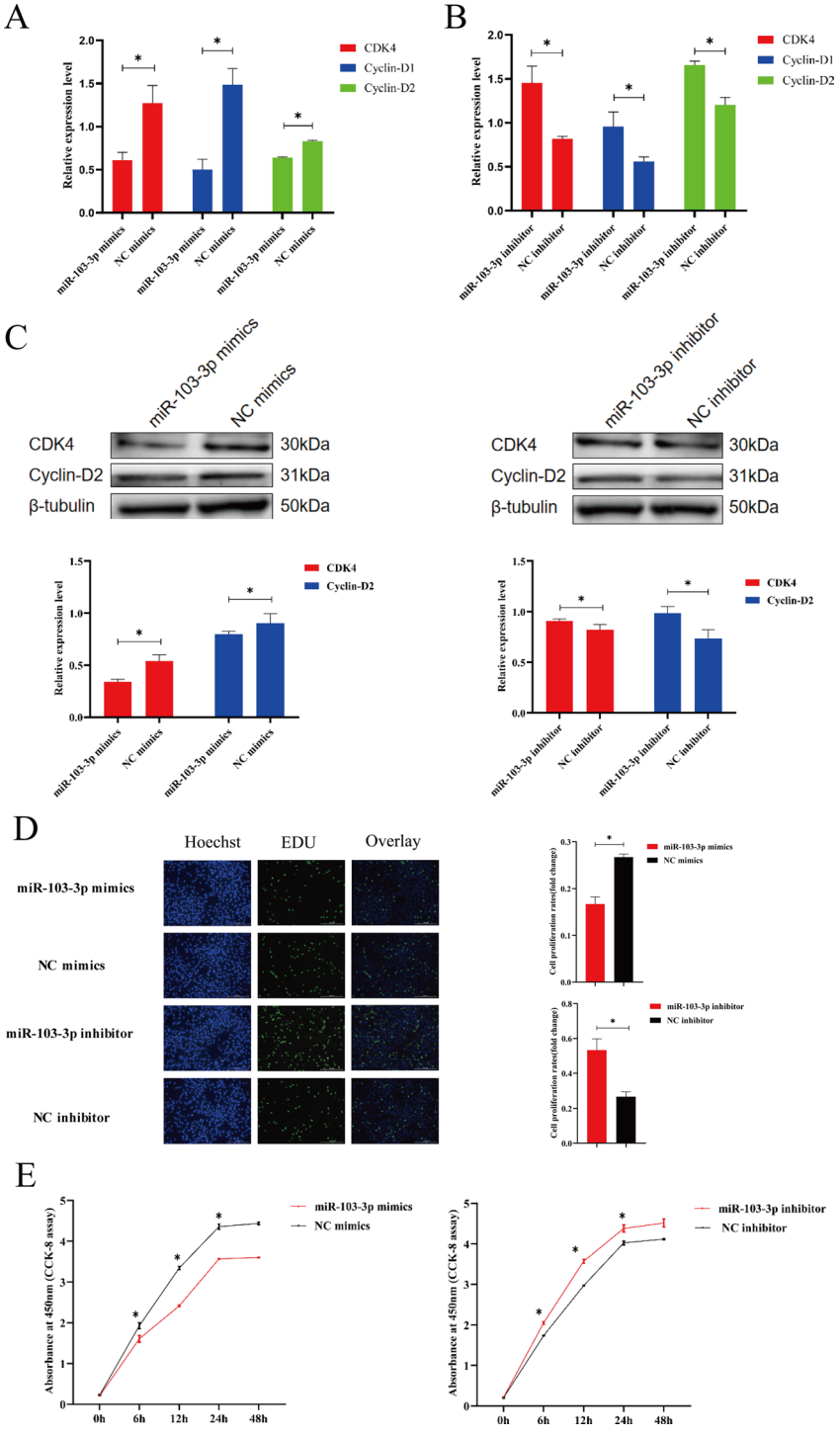

Fig. 4 The miR-103-3p inhibited the proliferation of goat myoblasts. (**A**) The relative expression of cell proliferation-related genes (*CDK4*, *CyclinD1* and *CyclinD2*) in the goat myoblasts after miR-103-3p overexpression. (**B**) The relative expression of cell proliferation-related genes (*CDK4*, *CyclinD1* and *CyclinD2*) in the goat myoblasts after miR-103-3p inhibition. (**C**) The protein levels of *CDK4* and *CyclinD2* in the goat myoblasts after miR-103-3p overexpression or inhibition. (**D**) EdU was used to detect the goat myoblast proliferation rate after miR-103-3p overexpression or inhibition. EdU (red), Hoechst (blue). (**E**) CCK-8 was used to determine the proliferation of myoblasts after miR-103-3p overexpression or inhibition. The bars represent the mean ± SEM of at least three replicates. * $P < 0.05$, ** $P < 0.01$

findings (Fig. 4C). Additionally, both CCK-8 and EdU assays demonstrated that overexpression of miR-103-3p markedly suppressed the proliferation rate of the goat myoblasts, with the opposite effect observed upon its inhibition (Fig. 4D and E). In summary, the results indicated that miR-103-3p significantly contributed to the suppression of goat myoblast proliferation.

FGF18/miR-103-3p targeting relationship validation and tissue expression analysis

One of the main functions of miRNAs is to repress the expression of their target genes by targeting the 3'UTR. Among the miRNA–mRNA interactions, *FGF18* was recognized as a target gene of miR-103-3p, a relationship pertinent to muscle fiber growth and development. Consequently, we selected this miRNA–mRNA pair for further functional validation. The expression patterns of *FGF18* and miR-103-3p in the *longissimus dorsi* tissues of 1-month-old and 9-month-old goats were examined using RT–qPCR and western blot analysis. The RT–qPCR data indicated an inverse correlation between *FGF18* expression and miR-103-3p levels in *longissimus dorsi* tissues (Fig. 5A), a finding that was supported by western blot analysis (Fig. 5B). To validate the binding between miR-103-3p and *FGF18*, we predicted the binding site and validated it using a dual-luciferase reporter assay. The prediction indicated that miR-103-3p could target the 3'UTR of *FGF18* (Fig. 5C). The dual luciferase assay demonstrated that miR-103-3p mimics significantly reduced the activity of the *FGF18* 3'UTR wild-type plasmid but had no effect on the activity of the mutant plasmid (Fig. 5D). Subsequently, we overexpressed or inhibited miR-103-3p in goat myoblasts and measured *FGF18* expression using RT–qPCR and western blotting. Overexpression of miR-103-3p led to a decrease in *FGF18* expression, whereas its inhibition resulted in an increase ($P<0.05$) (Fig. 5E), and the protein expression levels were consistent with the mRNA expression levels (Fig. 5F). Collectively, these findings suggested that miR-103-3p was inversely correlated with *FGF18* in goat *longissimus dorsi* tissues and could suppress *FGF18* expression in goat myoblasts.

FGF18 promoted the proliferation of goat myoblasts

To determine whether *FGF18* is a target gene of miR-103-3p that influences the proliferation of goat myoblasts, we created plasmids for the overexpression and inhibition of *FGF18* and assessed their effects through transfection experiments. Initially, we validated the efficacy of our constructed plasmids. Both RT-qPCR and western blot analyses confirmed that the overexpression of *FGF18* led to an increase in its expression in goat myoblasts, while its inhibition resulted in a decrease (Fig. 6A). Subsequently, RT-qPCR analysis of cell proliferation factors revealed that overexpression of *FGF18* in goat myoblasts led to a significant increase in the relative expression of *CDK4*, *Cyclin-D1*, and *Cyclin-D2*, with the opposite effect observed upon *FGF18* inhibition (Fig. 6B). Western blotting results corroborated the RT-qPCR findings (Fig. 6C). Additionally, both CCK-8 and EdU assays indicated that the proliferation rate of goat myoblasts significantly increased with *FGF18* overexpression but decreased with FGF18 inhibition ($P<0.05$) (Fig. 6D and E). Collectively, these results suggested that *FGF18* enhanced the proliferation of goat myoblasts and represented a pivotal pathway through which miR-103-3p suppressed the proliferation of these cells.

Discussion

MicroRNAs (miRNAs) are widely recognized for their role in regulating gene expression, especially at the posttranscriptional level. The miRNA transcriptome sequencing has become a prevalent tool for analyzing the molecular mechanisms underlying reproductive traits in livestock. According to transcriptome sequencing of Taurus skeletal muscle, miR-206, miR-1, miR-133, miR-12, and miR-17 were identified as the most abundant miRNAs [26]. Sequencing of the miRNA transcriptome in sheep skeletal muscle identified miR-1, miR-133, miR-181a, and miR-206 as the most abundantly expressed miRNAs [27]. Jaberin et al. showed that miR-1, miR-378, miR-133a, miR-26a, miR-26c, miR-378c and miR-199a-3p were the predominant miRNAs in the developing muscles of *C. melanogaster* [28]. These findings suggested substantial variation in miRNA expression levels within the skeletal muscle of various species. Nonetheless, the consistent high expression of certain miRNAs, including miR-1, miR-206, and miR-133, across species implies a potential essential role for these miRNAs in muscle growth and development in animals [29]. In our earlier research, we observed that the growth pattern of goat muscle fibers closely resembled that of sheep, with the fastest growth occurring at one month of age and a plateau occurring by adulthood at nine months of age [30, 31]. To explore the molecular mechanisms governing muscle fiber growth and development across various stages in goats, we profiled miRNA expression in the *longissimus dorsi* muscle tissues of goats at 1 month and 9 months of age through miRNA sequencing. In this research, we used q-value < 0.01 and |log2 (fold change) |>1 as the threshold for screening DE miRNAs, a criterion consistent with that used by Jia B et al. to screen DE miRNAs [29]. At the same time, we identified a total of 494 miRNAs, encompassing both known and novel miRNAs, with 448 miRNAs expressed at both developmental stages, albeit at varying levels between the mon1 and mon9 groups. Specifically, miR-103-5p, miR-106a-3p, and miR-346-5p were uniquely expressed in

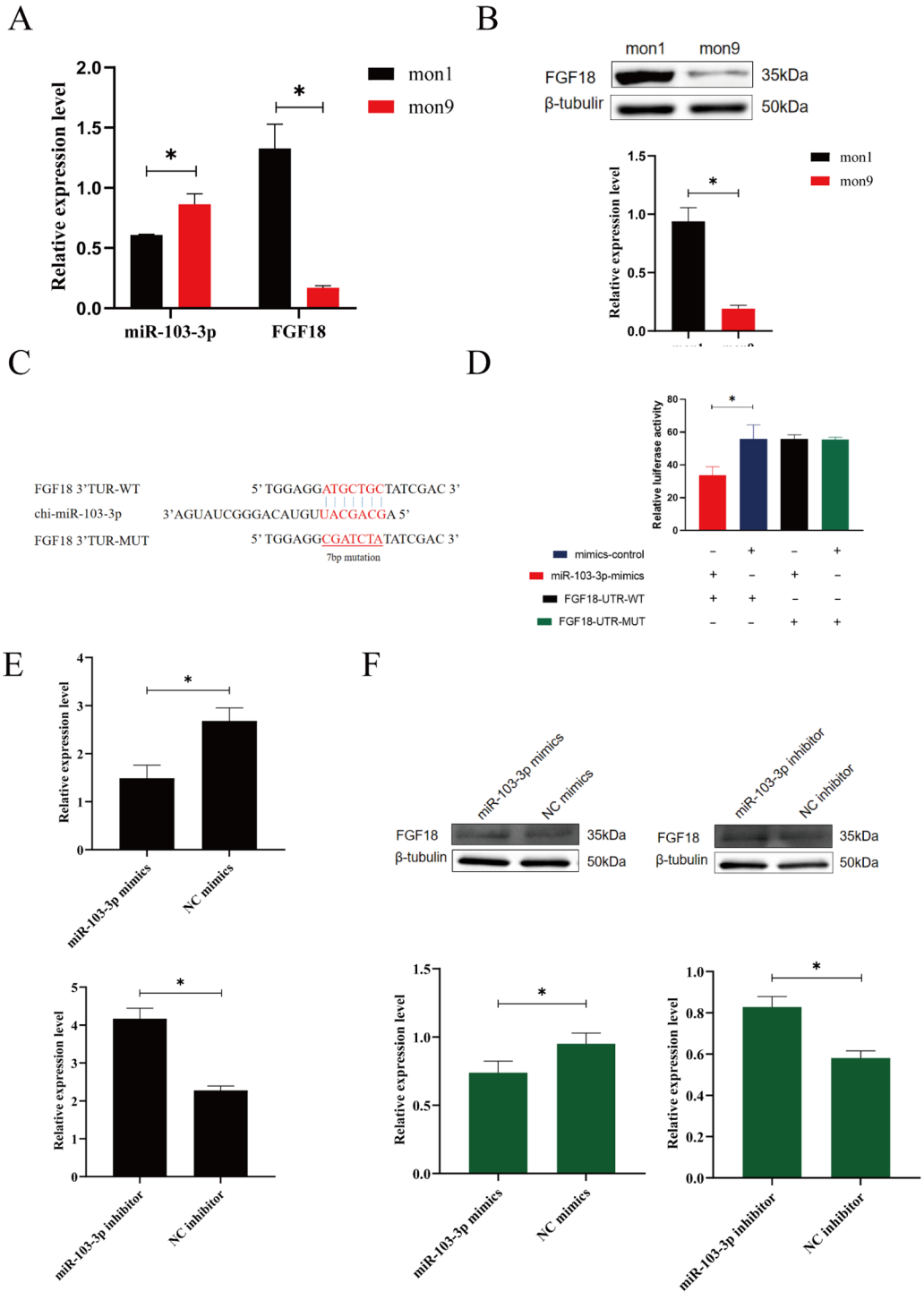

Fig. 5 Establishment of the interaction between miR-103-3p and *FGF18*. (**A**) Verification of the negative correlation between *FGF18* and miR-103-3p in the *longissimus dorsi* tissue of goats. (**B**) Detection of *FGF18* protein levels in the dorsal longissimus muscle tissues of goats at different growth stages. (**C**) Prediction of the binding site of chi-miR-103-3p to the 3′-UTR of *FGF*18. (**D**) Dual luciferase activity assay of miR-103-3p and the 3′-UTR of *FGF18*. (**E**) miR-103-3p inhibited the mRNA expression of *FGF18* in goat myoblasts. (**F**) miR-103-3p decreased the protein level of *FGF18* in goat myoblasts. * $P < 0.05$, ** $P < 0.01$

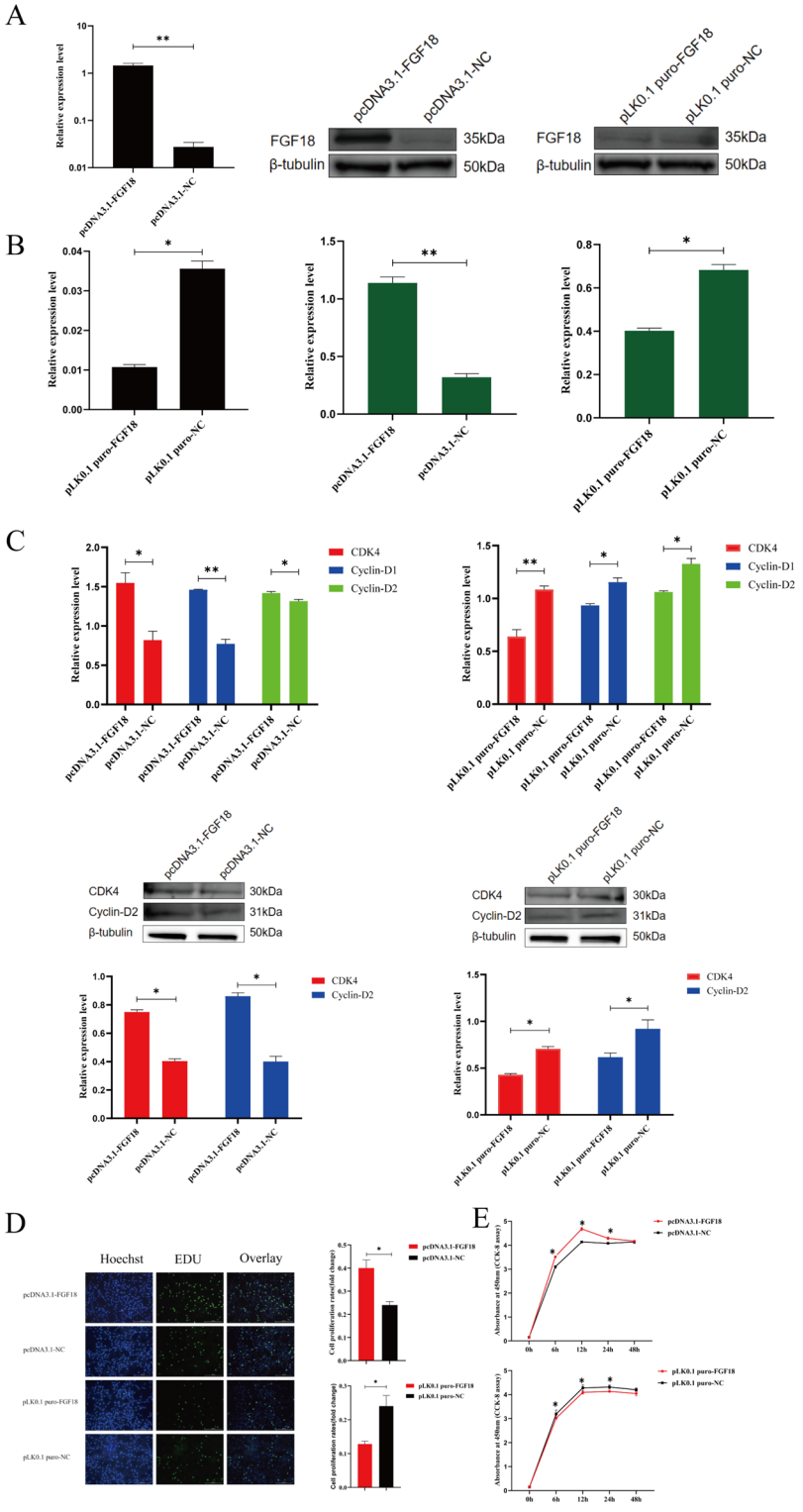

Fig. 6 *FGF18* enhanced the growth of goat myoblasts. (**A**) The expression of *FGF18* in goat myoblasts after *FGF18* overexpression or inhibition. (**B**) The relative expression of cell proliferation-related genes (*CDK4*, *CyclinD1* and *CyclinD2*) detected after *FGF18* overexpression or inhibition. (**C**) The protein levels of *CDK4* and *CyclinD2* were detected after *FGF18* overexpression or inhibition. (**D**) The EdU assay of goat myoblasts after *FGF18* overexpression or inhibition. EdU (red), Hoechst (blue). (**E**) CCK-8 assay of goat myoblasts after *FGF18* overexpression or inhibition. * $P < 0.05$, ** $P < 0.01$

the 1-month-old group (mon1), while miR-186-3p, miR-19b-5p, and miR-33b-5p were uniquely expressed in the 9-month-old group (mon9). It is hypothesized that these uniquely expressed miRNAs may play a role in muscle development or aging. These findings offer valuable insights for future research into the growth and developmental patterns of muscle myofibers and posttranscriptional regulatory mechanisms at different growth stages in goats.

Numerous studies have demonstrated that miRNAs are essential for controlling the development of skeletal muscle, either directly or indirectly. Specifically, miR-1 and miR-206 are known to modulate the proliferation and differentiation of skeletal muscle satellite cells by targeting Pax7, thereby impacting muscle growth and development. Additionally, miR-27b has been shown to influence these cellular processes by regulating the expression of the Pax3 protein, and miR-133 and miR-148a are also implicated in the regulation of skeletal muscle development [32]. In this study, we identified 32 differentially expressed miRNAs across various developmental stages. Notably, miRNAs implicated in the growth and development of muscle tissue, including miR-1, miR-206, and miR-22-5p, exhibited a gradual decrease in expression. Conversely, the levels of miRNAs associated with aging, such as miR-199a-5p [33], were significantly increased. These results were also consistent with previous studies showing that miRNAs with temporal or differential expression profiles are strongly related to muscle growth, maturation, and senescence [34]. The GO and KEGG analyses of the target genes of DEMs indicated that these genes are predominantly involved in the development of the organism, metabolic processes, material synthesis and energy transfer. We hypothesized that this correlation may be linked to the swift growth phase of goats between one and nine months of age, a period that demands substantial energy and resources for muscle development from the juvenile to adult stage. The 32 identified DEMs could be involved in these processes of material synthesis or energy transfer, warranting further investigation.

In biological systems, miRNAs orchestrate a vast array of processes by modulating their target genes within intricate networks. They facilitate the degradation of mRNA or inhibit its translation by binding complementarily to the 3' UTR of specific target mRNAs [35]. We established a network of miRNA–mRNA interactions relevant to goat muscle growth and development utilizing protein–protein interaction (PPI) data. This network encapsulates the sophisticated nature of muscle development in Wu'an goats. Within this intricate miRNA–mRNA interaction network, miR-103-3p has emerged as a central miRNA that orchestrates the regulation of multiple target genes, including *FGF18*, which is implicated in muscle growth and development. In this study, we confirmed the ability of miR-103-3p to bind to the 3'UTR region of *FGF18* by dual luciferase reporter assay. The miR-103-3p mimic had no effect on the activity of the mutant plasmid, but was able to significantly reduce the activity of the *FGF18* 3'UTR wild-type plasmid (Fig. 5C, D). RT-qPCR and western blotting also demonstrated that overexpression of miR-103-3p led to a decrease in *FGF18* expression, whereas inhibition of miR-103-3p led to an increase in *FGF18* expression (Fig. 5E, F). Studies have shown that miR-103-3p is an important regulator of myofibroblast proliferation and differentiation. For example, miR-103-3p regulates differentiation and autophagy of myoblasts by targeting *MAP4*, and miR-103-3p regulates proliferation and differentiation of C2C12 myoblasts by targeting *BTG2* [36, 37]. This is similar to the results of this study.

Consequently, the impact of this miRNA-mRNA axis on the proliferation of goat myoblasts was further investigated. *FGF18* belongs to the fibroblast growth factor (FGF) family, a group known for its 23 identified members that interact with five distinct FGF receptors. These receptors are characterized by an intracellular domain, a transmembrane segment, and an extracellular region [38, 39]. The FGF family plays a crucial role in a myriad of cellular and physiological processes in animals, including angiogenesis, cell differentiation and proliferation, tissue regeneration, morphogenesis, inflammatory responses, oncogenic transformation, and the development of both embryonic and skeletal systems [40–43]. In addition, members of the FGF family have been implicated in cell proliferation, migration, and invasion [44–46]. Research has demonstrated that *FGF18* is crucial for the processes of osteogenesis and chondrogenesis and is essential for maintaining normal cellular proliferation and differentiation [47]. Furthermore, *FGF18* is a secretory signaling molecule that plays an important role in embryonic development and osteogenic cartilage development [48–50]. *FGF18* significantly contributes to chondrocyte proliferation and differentiation and is also linked to the regulation of myogenesis [41–52]. Collectively, these findings indicate that *FGF18* is critically important for embryonic development, cellular proliferation and differentiation, and the formation of the skeletal system. Moreover, it exhibited a positive correlation with the developmental progress of skeletal muscle.

With the advent of the genome era, transcriptomics, which is the study of gene structure and function, has received more and more attention. By screening differentially expressed genes, we can link genes and traits and find target sites for genetic breeding. Researchers used RNA sequencing to generate miRNA-mRNA profiles of Leizhou goats, indicating that several miRNAs and mRNAs are involved in regulating muscle development

and growth in goats [53]. In Hu sheep, overexpression of miR-22-3p inhibits the proliferation of skeletal muscle cells and is involved in the proliferation and differentiation of skeletal muscle cells by targeting *IGFBP3* [54]. The above studies provide potential molecular loci for animal molecular breeding. Consequently, we undertook an in-depth investigation of *FGF18* and found that miR-103-3p significantly influences *FGF18* expression across various ages. Subsequent research revealed that miR-103-3p inhibits *FGF18* expression and markedly suppresses the proliferation of goat myoblasts. Considering the results of previous studies, we speculated that miR-103-3p may impede the proliferation of goat myoblasts by directly targeting *FGF18*, potentially influencing the development of goat skeletal muscle.

Conclusion

In summary, miRNA sequencing revealed the involvement of numerous miRNAs in the growth and development of myofibers within the *longissimus dorsi* tissue of goats. Notably, chi-miR-103-3p inhibited the proliferation of goat myoblasts by suppressing *FGF18* expression. The results from this study offer theoretical insights for future exploration of the molecular mechanisms that drive myofiber growth and development throughout the various stages of goat maturation.

Abbreviations

miRNA	microRNA
DE	Differentially expressed
3'UTR	3'untranslated region
mon1	1 month old
mon9	9 months old
GO	Gene Ontology
KEGG	Kyoto Encyclopedia of Genes and Genomes
RT	Reverse transcription
WT	Wild-type
MUT	Mutant
NC	Negative control
PBS	Phosphate-buffered saline
SE	Standard error
DEMs	Differentially expressed miRNAs
FPKM	Fragments per kilobase per million reads
TPM	Transcripts per kilobase per million reads
BP	Biological process
CC	Cellular component
MF	Molecular function

Supplementary Information

The online version contains supplementary material available at https://doi.org/10.1186/s12864-024-11183-4.

Supplementary Material 1

Supplementary Material 2

Supplementary Material 3: Table S1 FGF18 interference shRNA sequence. Table S2 All of the expressed miRNAs in the comparison. Table S3 Differentially expressed miRNAs. Table S4 DEMs and target–miRNA interaction analysis

Acknowledgements

Not applicable.

Author contributions

KL and YS were responsible for organizing the data, as well as writing-review and editing the manuscript, with KL being the primary contributor to the writing of the manuscript. YF and HZ utilized software for data analysis. MC and YL designed the overall experiment, secured funding, managed the project, and conducted the final review. All authors read and approved the final manuscript.

Funding

This research was funded by the Agricultural Science and Technology Innovation Program of China (ASTIP-IAS13), the China Agriculture Research System of MOF and MARA (CARS-38), and the Postdoctoral Fellowship Program of CPSF (GZC20233053).

Data availability

Data is provided within the manuscript or supplementary information files.

Declarations

Ethics approval and consent to participate

All the animals were authorized by the Science Research Department (in charge of animal welfare issue) of the Institute of Animal Science, Chinese Academy of Agricultural Sciences (IAS-CAAS, Beijing, China). In addition, ethical approval for animal survival was given by the animal ethics committee of IAS-CAAS (No. IAS 2022 – 128). Informed consent was obtained from the farm site for the sheep used in this trial.

Consent for publication

Not applicable.

Competing interests

The authors declare no competing interests.

Received: 14 June 2024 / Accepted: 23 December 2024
Published online: 07 January 2025

References

1. Stanišić N, Žujović M, Tomić Z, Maksimović N, Bijelić Z, Ivanović S, Memiši N. The effects of crossing Balkan and Saanen goat breeds on carcass traits and certain quality parameters of kid meat. Ann Anim Sci. 2012;12:53–62.
2. McMillin KW, Brock AP. Production practices and processing for value-added goat meat. J Anim Sci. 2005;83:E57–68.
3. Givens DI, Kliem KE, Gibbs RA. The role of meat as a source of n-3 polyunsaturated fatty acids in the human diet. Meat Sci. 2006;74:209–18.
4. Horcada A, Ripoll G, Alcalde MJ, Sañudo C, Teixeira A, Panea B. Fatty acid profile of three adipose depots in seven Spanish breeds of suckling kids. Meat Sci. 2012;92:89–96.
5. Ma GL, Xu HY. Comparative analysis of fat and protein content in goat meat and sheep meat produced in Inner Mongolia. Heilongjiang Anim Husb Veterinary Med, 2016, (10):87–8.
6. Wang SQ. Study on changes of structural characteristics of muscle fiber during development of Wuzhumuqin sheep. Hohhot: Inner Mongolia Agricultural University; 2012.
7. Wang YQ, Tian ZL, Shi HB, Zhong JL, Ren GY, Li YX, Liu YM, Wu QJ, Wang JP, Zhang ZQ, Ding K, Yu ZH, Zhao ZQ. Nutritional characteristics and muscle fiber histological characters of muscle from Hu Sheep. Chin J Anim Nutr. 2017;29(8):2867–74.
8. Wang J, Wang Q, Huang JX, Qi RL. Expression patterns and regulation mechanisms of microRNAs relate in growth and development of muscle in animals. Chin J Anim Nutr. 2017;29(8):2867–74.
9. Carrington JC, Ambros V. Role of microRNAs in plant and animal development. Science. 2003;301:336–8.
10. Rajewsky N. microRNA target predictions in animals. Nat Genet. 2006;38(Suppl):S8–13.

11. Chen JF, Tao Y, Li J, Deng Z, Yan Z, Xiao X, Wang DZ. microRNA-1 and microRNA-206 regulate skeletal muscle satellite cell proliferation and differentiation by repressing Pax7. J Cell Biol. 2010;190(5):867–79.
12. Huang MB, Xu H, Xie SJ, Zhou H, Qu LH. Insulin-like growth factor-1 receptor is regulated by microRNA-133 during skeletal myogenesis. PLoS ONE. 2011;6(12):e29173.
13. Chen X, Wang K, Chen J, Guo J, Yin Y, Cai X, Guo X, Wang G, Yang R, Zhu L, Zhang Y, Wang J, Xiang Y, Weng C, Zen K, Zhang J, Zhang CY. In vitro evidence suggests that miR-133a-mediated regulation of uncoupling protein 2 (UCP2) is an indispensable step in myogenic differentiation. J Biol Chem. 2009;284(8):5362–9.
14. Kong D, He M, Yang L, Zhou R, Yan YQ, Liang Y, Teng CB. MiR-17 and miR-19 cooperatively promote skeletal muscle cell differentiation. Cell Mol Life Sci. 2019;76:5041–54.
15. Zhao MJ, Xie J, Shu WJ, Wang HY, Bi J, Jiang W, Du HN. MiR-15b and miR-322 inhibit SETD3 expression to repress muscle cell differentiation. Cell Death Dis. 2019;10:183.
16. Wang J, Song C, Cao X, Li H, Cai H, Ma Y, Huang Y, Lan X, Lei C, Ma Y, Bai Y, Lin F, Chen H. MiR-208b regulates cell cycle and promotes skeletal muscle cell proliferation by targeting CDKN1A. J Cell Physiol. 2019;234:3720–9.
17. Mok GF, Lozano-Velasco E, Munsterberg A. MicroRNAs in skeletal muscle development. Semin Cell Dev Biol. 2017;72:67–76.
18. Dey BK, Gagan J, Yan Z, Dutta A. MiR-26a is required for skeletal muscle differentiation and regeneration in mice. Genes Dev. 2012;26:2180–91.
19. Lin CY, Chen JS, Loo MR, Hsiao CC, Chang WY, Tsai HJ. MicroRNA-3906 regulates fast muscle differentiation through modulating the target gene homer-1b in zebrafish embryos. PLoS ONE. 2013;8:e70187.
20. Lu C, Wu J, Xiong S, Zhang X, Zhang J, Mei J. MicroRNA-203a regulates fast muscle differentiation by targeting dmrt2a in zebrafish embryos. Gene. 2017;625:49–54.
21. Hu Z, Klein JD, Mitch WE, Zhang L, Martinez I, Wang XH. MicroRNA-29 induces cellular senescence in aging muscle through multiple signaling pathways. Aging. 2014;6:160–75.
22. Zacharewicz E, Della Gatta P, Reynolds J. Identification of microRNAs linked to regulators of muscle protein synthesis and regeneration in young and old skeletal muscle. PLoS ONE. 2014;9(12):e114009.
23. Mitchell CJ, D'Souza RF, Schierding W, Zeng N, Ramzan F, O'Sullivan JM, Poppitt SD, Cameron-Smith D. Identification of human skeletal muscle miRNA related to strength by high-throughput sequencing. Physiol Genomics. 2018;50(6):416–24.
24. Drummond MJ, McCarthy JJ, Sinha M, Spratt HM, Volpi E, Esser KA, Rasmussen BB. Aging and microRNA expression in human skeletal muscle: a microarray and bioinformatics analysis. Physiol Genomics. 2011;43(10):595–603.
25. Yao X, Gao X, Bao Y, El-Samahy MA, Yang J, Wang Z, Li X, Zhang G, Zhang Y, Liu W, Wang F. lncRNA FDNCR promotes apoptosis of granulosa cells by targeting the miR-543-3p/DCN/TGF-β signaling pathway in Hu sheep. Mol Ther Nucleic Acids. 2021;24:223–40.
26. McMillin Sun J, Li M, Li Z, Xue J, Lan X, Zhang C, Lei C, Chen H. Identification and profiling of conserved and novel microRNAs from Chinese Qinchuan bovine longissimus thoracis. BMC Genom. 2013;14:42.
27. Sheng X, Song X, Yu Y, Niu L, Li S, Li H, Wei C, Liu T, Zhang L, Du L. Characterization of microRNAs from sheep (*Ovis aries*) using computational and experimental analyses. Mol Biol Rep. 2011;38:3161–71.
28. Daza KR, Steibel JP, Velez-Irizarry D, Raney NE, Bates RO, Ernst CW. Profiling and characterization of a longissimus dorsi muscle microRNA dataset from an F2 duroc × pietrain pig resource population. Genom Data. 2017;13:50–3.
29. Jia B, Liu Y, Li Q, Zhang J, Ge C, Wang G, Chen G, Liu D, Yang F. Altered miRNA and mRNA expression in Sika deer skeletal muscle with age. Genes (Basel). 2020;11(2):172.
30. Zhou Z, Li K, Liu J, Zhang H, Fan Y, Chen Y, Han H, Yang J, Liu Y. Expression profile analysis to identify circular RNA expression signatures in muscle development of Wu'an goat longissimus dorsi tissues. Front Vet Sci. 2022;9:833946.
31. Liu Y, Zhou Z, Li K, Wang P, Chen Y, Deng S, Li W, Yu K, Wang K. VMP1 regulated by chi-miR-124a effects goat myoblast proliferation, autophagy, and apoptosis through the PI3K/ULK1/mTOR signaling pathway. Cells. 2022;11:2227.
32. Mitchelson KR, Qin WY. Roles of the canonical myomiRs miR-1, -133 and –206 in cell development and disease. World J Biol Chem. 2015;6(3):162–208.
33. Hashemi Gheinani A, Burkhard FC, Rehrauer H, Aquino Fournier C, Monastyrskaya K. MicroRNA miR-199a-5p regulates smooth muscle cell proliferation and morphology by targeting WNT2 signaling pathway. J Biol Chem. 2015;290(11):7067–86.
34. Zhu L, Hou L, Ou J, Xu G, Jiang F, Hu C, Wang C. MiR-199b represses porcine muscle satellite cells proliferation by targeting JAG1. Gene. 2019;691:24–33.
35. Williams AH, Liu N, van Rooij E, Olson EN. MicroRNA control of muscle development and disease. Curr Opin Cell Biol. 2009;21(3):461–9.
36. He Y, Yang P, Yuan T, Zhang L, Yang G, Jin J, Yu T. *miR-103-3p* Regulates the Proliferation and Differentiation of C2C12 Myoblasts by Targeting BTG2. Int J Mol Sci. 2023;24(20):15318.
37. Zhang X, Huang S, Niu X, Li S, Wang J, Ran X. miR-103-3p Regulates the Differentiation and Autophagy of Myoblasts by Targeting MAP4. Int J Mol Sci. 2023;24(4):4130.
38. Kim JY, Park YK, Lee KP, Lee SM, Kang TW, Kim HJ, Dho SH, Kim SY, Kwon KS. Genome-wide profiling of the microRNA-mRNA regulatory network in skeletal muscle with aging. Aging. 2014;6:524–44.
39. Oulion S, Bertrand S, Escriva H. Evolution of the FGF gene family. Int J Evol Biol. 2012;2012:298147.
40. Del Diez R, Morales AV. The multiple roles of FGF signaling in the developing spinal cord. Front Cell Dev Biol. 2017;5:58.
41. Majidinia M, Sadeghpour A, Yousefi B. The roles of signaling pathways in bone repair and regeneration. J Cell Physiol. 2018;233(4):2937–48.
42. Itoh N, Ornitz DM. Evolution of the Fgf and Fgfr gene families. Trends Genet. 2004;20(11):563–9.
43. Presta M, Chiodelli P, Giacomini A, Rusnati M, Ronca R. Fibroblast growth factors (FGFs) in cancer: FGF traps as a new therapeutic approach. Pharmacol Ther. 2017;179:171–87.
44. Feng S, Wang J, Zhang Y, Creighton CJ, Ittmann M. FGF23 promotes prostate cancer progression. Oncotarget. 2015;6(19):17291–301.
45. Elo T, Lindfors PH, Lan Q, Voutilainen M, Trela E, Ohlsson C, Huh SH, Ornitz DM, Poutanen M, Howard BA, Mikkola ML. Ectodysplasin target gene Fgf20 regulates mammary bud growth and ductal invasion and branching during puberty. Sci Rep. 2017;7(1):5049.
46. Wu XL, Gu MM, Huang L, Liu XS, Zhang HX, Ding XY, Xu JQ, Cui B, Wang L, Lu SY, Chen XY, Zhang HG, Huang W, Yuan WT, Yang JM, Gu Q, Fei J, Chen Z, Yuan ZM, Wang ZG. Multiple synostoses syndrome is due to a missense mutation in exon 2 of FGF9 gene. Am J Hum Genet. 2009;85(1):53–63.
47. Ohbayashi N, Shibayama M, Kurotaki Y, Imanishi M, Fujimori T, Itoh N, Takada S. FGF18 is required for normal cell proliferation and differentiation during osteogenesis and chondrogenesis. Genes Dev. 2002;16(7):870–9.
48. Lavranos TC, Rodgers HF, Bertoncello I, Rodgers RJ. Anchorage-independent culture of bovine granulosa cells: the effects of basic fibroblast growth factor and dibutyryl cAMP on cell division and differentiation. Exp Cell Res. 1994;211:245–51.
49. Buratini J Jr, Teixeira AB, Costa IB, Glapinski VF, Pinto MG, Giometti IC, Barros CM, Cao M, Nicola ES, Price CA. Expression of fibroblast growth factor-8 and regulation of cognate receptors, fibroblast growth factor receptor-3c and – 4, in bovine antral follicles. Reproduction. 2005;130(3):343–50.
50. Yue M, Lan Y, Liu H, Wu Z, Imamura T, Jiang R. Tissue-specific analysis of Fgf18 gene function in palate development. Dev Dyn. 2021;250(4):562–73.
51. Lim RW, Hauschka SD. A rapid decrease in epidermal growth factor-binding capacity accompanies the terminal differentiation of mouse myoblasts in vitro. J Cell Biol. 1984;98(2):739–47.
52. Liu Z, Lavine KJ, Hung IH, Ornitz DM. FGF18 is required for early chondrocyte proliferation, hypertrophy and vascular invasion of the growth plate. Dev Biol. 2007;302(1):80–91.
53. Fu J, Liu J, Zou X, Deng M, Liu G, Sun B, Guo Y, Liu D, Li Y. Transcriptome analysis of mRNA and miRNA in the development of LeiZhou goat muscles. Sci Rep. 2024;14(1):9858.
54. Wang S, Cao X, Ge L, Gu Y, Lv X, Getachew T, Mwacharo JM, Haile A, Sun W. MiR-22-3p Inhibits Proliferation and Promotes Differentiation of Skeletal Muscle Cells by Targeting IGFBP3 in Hu Sheep. Anim (Basel). 2022;12(1):114.

Publisher's note